Activation of the Crtc2/Creb1 transcriptional network in skeletal muscle enhances weight loss during intermittent fasting

Nelson E. Bruno[1]*, Jerome C. Nwachukwu[1], Sathish Srinivasan[1], Richard Hawkins, David Sturgill[3], Gordon L. Hager[3], Stephen Hurst[4], Shey-Shing Sheu[4], Michael D. Conkright[5], Kendall W. Nettles[1]*

[1]Department of Integrative Structural and Computational Biology, The Scripps Research Institute, 130 Scripps Way, Jupiter FL 33458, USA

[2]Department of Cancer Biology, The Scripps Research Institute, 130 Scripps Way, Jupiter FL 33458, USA

[3]Laboratory of Receptor Biology and Gene Expression, National Cancer Institute, NIH, Bethesda, MD 20892, USA

[4]Center for Translational Medicine, Department of Medicine, Thomas Jefferson University, Philadelphia, PA, 19107, USA.

[5]Department of Shared Services, The Scripps Research Institute, 130 Scripps Way, Jupiter FL 33458, USA

Correspondence: Nelson E Bruno, nbruno@scripps.edu; Kendall Nettles, knettles@scripps.edu

Competing interest statement: The authors declare no competing interests.

Abstract

Exercise is a behavior modification indispensable for long-term weight loss. Exercise activates the Creb-Regulated Transcriptional Coactivator (Crtc) family of transcriptional coregulators to drive Creb1-mediated anabolic transcriptional programs in skeletal muscle. Here, we show that induced overexpression of a skeletal muscle specific Crtc2 transgene in aged mice leads to greater weight loss during alternate day fasting, and selective loss of fat rather than lean mass. Transcriptional profiling revealed that fasting and weight loss downregulated most of the mitochondrial electron transport genes and other regulators of mitochondrial function that were substantially reversed in the Crtc2 mice, which maintained higher energy expenditure during fasting. The Crtc2 mice displayed greater mitochondrial activity, metabolic flux capacity for both carbohydrates and fats, improved glucose tolerance and insulin sensitivity, and increased oxidative capacity before the fast, suggesting muscle-intrinsic mechanisms in support of improved weight loss. This work reveals that Crtc2/Creb1-mediated signaling coordinates metabolic adaptations in skeletal muscle that explain how Crtc2/Creb contribute to the effects of exercise on metabolism and weight loss.

Introduction

Long-term dieting is usually not effective in maintaining a lower body weight due to increased hunger and a slower metabolic rate (1). In humans, loss of >10% of body weight also increases metabolic efficiency, such that ~500 less calories per day are required to maintain the same energy expenditure (2). Weight loss reduces the metabolic rate due to a number of changes including increased circulating leptin and decreased thyroid hormone and sympathetic nervous system (SNS) activity (2-4). People who maintain long-term weight loss almost invariably exercise (5), and both preclinical and clinical data suggest that this is through raising metabolic rate (6-8), decreased energy efficiency (9), and increased energy expenditure from the increased physical activity (10).

Creb1-regulated transcription is stimulated by GPCRs that activate adenylyl cyclases to convert ATP to the second messenger cAMP, which in turn liberates the catalytic subunit of protein kinase A (PKA) (11). Crtc1–3 family members are primary coactivators for Creb1 that are also highly conserved in the cAMP transcriptional response. Crtc1–3 are rendered cytoplasmic and inactive by phosphorylation (12). In contrast, they are fully activated through synergistic dephosphorylation by phosphatases downstream of PKA and calcium flux in polarizable tissues including the skeletal muscle (13), hippocampus (14), cortex (15), islet cells (12), and the renal proximal tubule (16).

To study the effects of Crtc2/Creb1 activation in adult skeletal muscle, we generated doxycycline (dox)-inducible transgenic mice that show skeletal muscle-specific overexpression of Crtc2 under the control of a tetracycline response element (13). C57BL/6-Tg(TRE-Crtc2tm)1Mdc/j mice express the FLAG-Crtc2 S171A/S275A/K628R mutant attenuating the phosphorylation-driven negative feedback loop that exports Crtc2 from the nucleus to the cytoplasm. These mice were crossed with the C57BL/6-Tg 1256[3Emut] MCK-rtTA mice that

60 express the reverse tetracycline transactivator (rtTA) specifically in skeletal muscle to control
61 spatial expression limited to the skeletal muscle compartment (Grill *et al*, 2003). We identified a
62 double transgenic line with expression that was tightly regulated by dox and highly selective for
63 skeletal muscle, that we refer to as Crtc2 mice. These mice showed an exercised phenotype
64 including induction of *Ppargc1a*/PGC-1α and other anabolic genes, increased glycogen and
65 intramuscular triglycerides (IMTGs), increased muscle cross sectional area, and a remarkable
66 increase in high intensity exercise performance after less than two weeks of transgene induction
67 (13). Activation of Crtc2/Creb1 after exercise has now been demonstrated a number of times in
68 humans, but may depend on the type, duration, and intensity of exercise to upregulate anabolic
69 genes (17-20).

70 Given the primary role of exercise adaptations in regulating whole-body metabolism, we
71 examined here the role of the Crtc2/Creb1 transcriptional network in skeletal muscle metabolism
72 during alternate day fasting (ADF), mimicking a common dieting scheme in humans. Activation
73 of Creb1-regulated transcriptional responses during fasting enabled maintenance of a lower body
74 weight due to the stimulation of higher energy expenditure and other metabolic changes, enabling
75 selective loss of fat mass and retention of lean mass, as observed in humans who exercise (21, 22).
76 Transcriptional profiling revealed that ADF reduced the expression of most mitochondrial
77 respiratory chain subunits and lowered energy expenditure, which was prevented by modest Crtc2
78 overexpression. Crtc2 mice displayed the metabolic hallmarks of an exercised phenotype,
79 including enhanced mitochondrial activity, improved lipid and carbohydrate flux capacity and
80 storage, and insulin sensitization. These data support a model where lower metabolic activity
81 during fasting and weight loss contributes to weight regain, which can be reversed by exercise-
82 induced activation of Crtc2/Creb1-regulated transcriptional programs.

83

84 **Results**

85 **Crtc2 overexpression in skeletal muscle facilitates weight loss**

86 We studied aged Crtc2 (rtTA/Crtc2^{tm}) or WT (rtTA/WT) mice, which in the C57BL/6 background
87 naturally gain fat mass as they age (18 weeks, 30–39 g, **Figure 1A–B**). During dox treatment,
88 Crtc2 mice gained weight similarly to control WT mice (SI Appendix, **Figure S1A**). On the ADF
89 protocol, three separate cohorts of Crtc2 mice displayed significantly greater and sustained weight
90 loss than WT mice, with Crtc2 mice losing about twice as much weight in each case, 9-14% of
91 body weight (**Figure 1C, Figure S1B**).

92 After 3 weeks of ad libitum refeeding, the Crtc2 mice re-gained more weight to catch up
93 with the WT mice (**Figure 1D**), which may be due to the anabolic effects of higher insulin
94 sensitivity, described below. We also completed behavioral profiling studies and found that
95 locomotion was similarly reduced in both groups during the refeeding period (**Figure S1C**).
96 During the refeeding period the number of meals doubled in both groups, while meal duration and
97 number of bouts per meal declined (**Figure 1E**). We observed a reduction in kilocalories consumed
98 in the Crtc2 relative to the WT group, which planned comparisons demonstrated was significant
99 only during the second ADF cycle, when the WT mice increased consumption at a faster rate than
100 the Crtc2 mice (**Figure 1E**). These differences in caloric consumption are consistent with the
101 differences in body weight between cohorts and disappear after normalization for body weight.
102 Control mice lost more lean mass, while Crtc2 mice conserved lean mass and burned the excess
103 fat accumulated during aging (**Figure 1F**). To verify that Crtc2 helps maintain lower body weight
104 in a different model, we placed mice on a high fat diet, and found that Crtc2 mice also maintained
105 lower body weight than WT mice in this context (**Figure 1G**). Thus, the activation of Crtc2/Creb1

106 signaling in skeletal muscle significantly modulated body composition and weight loss.

107

108 **The transcriptional response to fasting and weight loss and its regulation by Crtc2**

109 To understand the skeletal muscle intrinsic effects of Crtc2 on dieting and weight loss, we performed
110 transcriptional profiling of mice tibialis anterior (TA) muscles electroporated with control and Crtc2
111 expression plasmids in contralateral legs. One cohort of electroporated mice was subject to 3 cycles
112 of ADF, while the other cohort was fed ad libitum. TA muscle tissues were collected from both
113 cohorts at the end of the third 24-hr fast. The transduction increased *Crtc2* mRNA levels by ~2.5-
114 fold across groups (**Figure 2A**). In response to ADF, we identified 1,880 differentially expressed
115 genes (DEGs) in the control-transduced muscle and 3,197 DEGs in Crtc2-transduced muscle, with
116 1,380 genes in common between the two groups (**Figure 2B**). Analysis of canonical signaling
117 pathways and gene ontology (GO) annotations revealed that ADF modulated the transcriptional
118 programs for lipid and carbohydrate metabolism, fatty acid beta-oxidation, and insulin signaling
119 (**Figure 2C-D**). ADF also regulated transcriptional programs that control protein balance, including
120 autophagy and ubiquitin-dependent proteasomal degradation which were upregulated, RNA
121 splicing, and transcription (**Figure 2C-D**).

122 To understand other transcriptional control mechanisms underlying the skeletal muscle
123 response to fasting and weight loss, we examined genes annotated as transcription factors or
124 transcriptional coregulators and found over 200 DEGs regulated by ADF. These include the
125 upregulation of a cohort of nuclear receptors that control energy expenditure, lipid metabolism and
126 mitochondrial function (*Thra*, *Nr4a3, PPARs, RXRα, RORα*) (**Figure 2E**) (23). Mice lacking *Nr2c2*
127 (TR4) display abnormal mitochondrial composition and function (24), but its role in the fasting and
128 weight loss is not known. As expected by their roles in coordinating the skeletal muscle atrophy, we

129 observed upregulation of the *Foxo3* and *Foxo4* transcription factor genes following ADF (**Figure**
130 **2F**). We also observed upregulation of the *Foxn3* gene which regulates hepatic glucose homeostasis,
131 but whose role in skeletal muscle is unknown (25). We identified a number of transcription factors
132 implicated in myoblast differentiation and regeneration (*Foxk1*, *Nfix*, *Klf9*, *Vgll2*, *Peg3*, *Sox7*),
133 suggesting they may play additional roles in the skeletal muscle response to fasting and weight loss.
134 The 85 transcriptional coregulators with ADF-dependent changes in expression, include
135 histone acetyltransferases, corepressors, chromodomain proteins, protein methyltransferases and
136 demethylases (**Figure 2G**). For example, Carm1 is a methyltransferase required for the effects of
137 Foxo3 on atrophy (26), and the histone deacetylases Hdac2, Hdac3, and Hdac7, have broad roles in
138 skeletal muscle physiology (27, 28). *Prkcb*/PKCβ was upregulated by ADF, and in addition to its
139 role as a transcriptional coregulator, PKCβ phosphorylates and inhibits the insulin receptor to inhibit
140 its activity (29), and activates the generator of mitochondrial ROS, p66shc (30).
141 Overexpression of Crtc2 in the context of ADF altered expression of 42 transcription factors
142 and 15 coregulators. These include the nuclear receptor, ERRα, which regulates mitochondrial
143 biogenesis, and RXRβ. RXRs are the obligate heterodimer partner for TR and PPARs. *E2F6*, which
144 causes cardiac hypertrophy upon overexpression (31), was upregulated by ADF only in the Crtc2
145 condition. However, 74% of Crtc2-dependent DEGs that encode transcription factors were inhibited,
146 including myogenin, a primary driver of atrophy, and *Irf1*, *Irf7*, *Notch2*, and *Stat1,* which control
147 immune and inflammatory responses. Crtc2 also inhibited many other genes implicated in the
148 inflammatory response including the nuclear factor-kappa B (NF-κB) signaling pathway. These
149 findings demonstrate that ADF and its associated weight loss profoundly changes the expression of
150 transcriptional regulators in skeletal muscle, effects significantly modulated by Crtc2.
151

152 **Crtc2 reverses fasting- and weight loss-induced effects on mitochondria and energy**
153 **expenditure**

154 In addition to lower metabolic rate, fasting and weight loss render humans and other mammals more
155 energetically efficient, such that the same amount of work is performed with less ATP production,
156 suggesting a remodeling of glycolytic or oxidative capacity (2, 32). ADF modulated the expression
157 of >200 genes whose proteins localize in mitochondria according to MitoCarta (33) (**Figure 3A**).
158 ADF downregulated most of the genes that encode the electron transport chain (complexes I–IV),
159 the ATP synthase (complex V), the mitoribosome, and the cytosolic ribosome (**Figure 3A-C**, **Figure**
160 **S3A**), but significantly upregulated genes such as *Sdha*, *Uqcrc1*, and *Atp5a1* (**Figure 3B**, **Figure**
161 **S3A**).

162 We observed a significant ADF-induced expression of genes encoding ROS scavenger
163 proteins such as thioredoxin (*Txnrd1*) and catalase (*Cat*), and genes regulating mitochondrial
164 stability*, Tomm7, Timm9,* and the AAA protease *Spg,7* known to be active during the removal of
165 damaged mitochondrial proteins (**Figure 3D**). Among the ATP synthase genes, there was a more
166 pronounced loss of gene expression in the lateral stalk genes (**Figure 3B**), which may decrease the
167 conductance of mitochondrial permeability transition pore (mPTP) and thus protect mitochondria
168 from detrimental swelling and oxidative injury (34). ADF also induced increases in mitochondrial
169 fusion (*Mfn2* and *Opa1)*, and decreased fission (*Fis)* gene expression, consistent with the protective
170 effects of fusion during nutrient deprivation (35). These adaptations could be advantageous for
171 weight loss as it prepares the mitochondria for the reduced metabolic rate and increased reliance on
172 lipid metabolism during fasting, without causing permanent damage to the mitochondrial pool within
173 the cell.

174 In mice subjected to ADF, Crtc2 transduction altered expression of 80 genes whose proteins

175 localize in the mitochondria. Crtc2 expression strongly attenuated the ADF-dependent repression of
176 electron transport chain genes and the mitoribosome (**Figure 3A–C**, **Figure S3A**), and generally
177 upregulated the other genes encoding proteins that localize to mitochondria. In addition, Crtc2
178 enhanced expression of ribosomal genes that facilitate mitoribosome assembly, and genes such as
179 *Spg7, Pink1, RhoT2*, and *Chchd3* that control the quality of mitochondrial proteins, but blocked
180 ADF-dependent downregulation of *Minos1*, a central component of the mitochondrial inner
181 membrane organizing system (**Figure 3D**). Crtc2 also upregulated expression of *Tefm*, the
182 mitochondrial transcriptional elongation factor, and *Bola3*, which participates in electron transport
183 chain assembly (36).

184 To understand how ADF affects mitochondria, we noted that glucocorticoids (GCs) are
185 one of the primary drivers of catabolic changes during fasting, and in response to ADF and Crtc2
186 overexpression, we observed over a thousand DEGs that were annotated as "glucocorticoid
187 response" genes (**Figure 2C**). In the context of an overnight fast, treatment with Dex more than
188 doubled loss of lean mass (**Figure 3E**). Using high-content imaging, we observed that Dex reduced
189 the diameter and mitochondrial potential of nutrient-deprived primary mouse skeletal myotubes
190 (**Figure 3F**). GCs can also activate the master energy sensor, AMP-activated protein kinase
191 (AMPK) (37), which can act as a glucocorticoid receptor (GR) coactivator (38). AMPK is
192 activated by a lower ATP/ADP ratio during fasting to inhibit anabolism and stimulate catabolic
193 processes such as autophagy and mitophagy. In primary myotubes, we observed a Dex-dependent
194 activating phosphorylation of AMPK that increased over time, consistent with an underlying
195 transcriptional mechanism (**Figure 3G**). Activation of AMPK with both Dex and the AMP analog,
196 AICAR, had an additive detrimental effect on myotube diameter (**Figure 4H**), suggesting that GR
197 collaborates with AMPK to drive skeletal muscle atrophy.

198 We also observed that ADF modulated the expression of genes encoding three of the
199 AMPK subunits. Changes in subunit composition are known to alter the regulation, substrate
200 preferences, and cellular location of AMPK. The α2 and β2 AMPK isoforms were significantly
201 upregulated by ADF (SI Appendix, **Figure 3I**). The α2 subunit is activated by low glycogen and
202 mediating nuclear translocation (39), while the β2 subunit is required for maintenance of muscle
203 ATP levels during fasting (40). In contrast, ADF downregulated the γ3 AMPK isoform (**Figure**
204 **3I**), which is required for glycogen synthesis (41), a process inhibited during fasting. Thus, a
205 combination of GR and AMPK signaling drives skeletal muscle atrophy during nutrient
206 deprivation and a loss of mitochondrial potential.

207 We further examined whether ADF- and Crtc2-induced changes in mitochondria—the
208 powerhouse of cellular respiration—are associated with changes in global energy expenditure. As
209 expected, ad libitum oxygen consumption cycled with activity in the mice, which increased at
210 night and decreased during the day (**Figure 3J, Figure S3B**). Fasting reduced oxygen consumption
211 at every cycle, and this effect was more pronounced during the day as the fast was extended
212 (**Figure S3B**). However, Crtc2 mice consistently showed higher oxygen consumption,
213 independent of fasting (**Figure 2J**).

214 When fed ad libitum, Crtc2 and control mice display similar rates of energy expenditure
215 (EE) (**Figure 3JK**). We calculated EE from indirect calorimetry measurements of VO_2 and VCO_2
216 and performed ANCOVA analysis using body weight and NMR data as covariates to adjust the
217 EE to total body weight and body composition (**Figure S3C**). While fasting, the EE of WT mice
218 dropped significantly. In contrast, during fasting EE in Crtc2 mice did not drop below the ad
219 libitum levels (**Figure 3I**). Respiratory quotient was also reduced during fasting, indicating greater
220 utilization of fat for fuel, but the differences between WT and Crtc2 mice were not significant

221 (**Figure S3D–E**). These data suggest potential mechanisms to explain how physical activity—
222 through Crtc2/Creb1-regulated transcriptional programs—can help maintain a higher metabolic
223 rate and a lower body weight by upregulating expression of mitochondrial respiratory chain subunits
224 and modulating expression of other mitochondria-localized gene products, consistent with the well-
225 known beneficial effects of exercise on mitochondrial biogenesis and quality control.
226

227 **Crtc2 stimulates mitochondrial activity and improves oxidative capacity**

228 Prolonged fasting promotes lipolysis, insulin resistance, and mobilization of fatty acids to skeletal
229 muscle through the combined effects of glucagon and glucocorticoids on adipocytes. These actions
230 augment the rate of fatty acid oxidation by mitochondria and the ectopic accumulation of IMTGs.
231 As expected, ADF upregulated a panoply of genes involved in the transport, oxidation, and
232 esterification of fatty acids. Key among these are: *Ppard* and *Ppara,* the chief regulators of fat
233 metabolism in muscle; *Cd36* that regulates plasma membrane fatty acid transport and utilization
234 to spare glucose; *Ucp3,* which is implicated in β-oxidation as well as protection from triglyceride
235 accumulation in muscle (42); *Pdk2* and *Pdk4,* which promote fatty acid oxidation over glycolysis
236 (43); and multiple enzymes involved in Acyl-CoA metabolism (**Figure 4A**). *Acox1* is a
237 peroxisomal Acyl-CoA oxidase, while *Acad10*, *Acadl*, *Acadm* are members of the acyl-coenzyme
238 A dehydrogenase family that are critical for effective beta-oxidation in the mitochondria. *Acsl1*,
239 *Acot1*, *Acot2*, and *Acot4* regulate the generation and hydrolysis of Acyl-CoA. Differential
240 expression of *Dgat2*, *Daglb*, *Plin5* and other genes that regulate lipid storage and accumulation
241 highlights their importance in lipid homeostasis during fasting. Notably, the lipoprotein lipase
242 (*Lpl*) gene, which controls a rate limiting step in lipoprotein metabolism, was upregulated by ADF
243 more robustly in Crtc2-transduced legs than in control legs, suggesting an improved post prandial

244 metabolism of triglyceride-rich lipid particles. *Sirt4*, a mitochondrial sirtuin that regulates the rate
245 of fatty acid oxidation in muscle, was also substantially suppressed during fasting but significantly
246 less so in the Crtc2-overexpressing legs which may favor the higher lipid accumulation that we
247 previously described in muscle overexpressing Crtc2 (13).

248 Crtc2 mice displayed higher oxygen consumption before the fast; therefore, we examined
249 them for improved mitochondrial function. After one week of dox treatment, Crtc2 mice showed
250 increased mitochondrial succinate dehydrogenase activity in the gastrocnemius muscle (**Figure 4B,**
251 **Figure S4A–B**) and increased expression of *Cytochrome C (Cycs)* (**Figure 4C**). In addition to the
252 previously reported upregulation of *Ppargc1a/*PGC-1α (13), Crtc2 mice showed increased
253 expression of *Nr4a3/*NOR-1, a nuclear receptor family transcriptional factor (**Figure 4C**). PGC-
254 1α and NOR-1 induce mitochondrial biogenesis and increase oxidative capacity (44, 45). Crtc2
255 also upregulated the *Dgat1* gene (**Figure 4C**), which is a direct Creb1 target gene (13), the product
256 of which catalyzes a rate-limiting step that increases IMTG stores. These mitochondria-related
257 genes were also upregulated in primary myotubes overexpressing Crtc2, indicating a skeletal
258 muscle-intrinsic effect of Crtc2 that mimics the effects of exercise (**Figure 4D**). To show that
259 Creb1 is directly regulating atrophy, we transduced primary myocytes with the dominant negative
260 A-Creb, which reduced myotube diameter (**Figure 4E**). We also observed a doubling of
261 mitochondrial DNA after in vivo electroporation of Crtc2 (**Figure 4F**). The increased
262 mitochondrial mass was associated with increased oxidative capacity, as myotubes overexpressing
263 Crtc2 or Crtc3 oxidized more palmitate than control myotubes (**Figure 4G**), as previously reported
264 (46).

265

266 **Crtc2 improved glucose tolerance and carbohydrate metabolism before and during weight loss**

267 During fasting, the rise of non-esterified fatty acid levels in plasma leads to a suppression of insulin
268 signaling and glucose metabolism in skeletal muscle, where glycogen levels can drop by ~40% (47).
269 After 3 cycles of ADF, we found a significant activation of genes involved in glycogen metabolic
270 processes, including synthesis (*Gys1*, *Fbp2*, *Ugp2*, *Epm2a*, and *Ppp1cb*), branching (*Gbe1*), and
271 breakdown (*Gaa*, *Agl*, *Gsk3b*) of glycogen, perhaps in preparation for feeding (**Figure 5A**).
272 Likewise, a number of genes involved in different aspects of insulin signaling were also activated
273 in both Crtc2-transduced and control muscle, including *Irs2*, *Sorbs1,* and *Insr*. Many genes
274 necessary for glycolysis and fructose metabolism were suppressed by ADF, including *Pfkfb1,*
275 *Pfkfb2*, and *Fuk*. *Ogt*, an important inducer of insulin resistance in skeletal muscle via the inhibition
276 of AKT phosphorylation was also downregulated.

277 To probe for Crtc2-dependent changes in carbohydrate metabolism, we performed glucose
278 tolerance tests comparing Crtc2 and WT mice following ADF or normal diet. The Crtc2 mice
279 displayed significantly improved glucose disposal after ADF, including a dramatic improvement in
280 their ability to reduce glycemia (**Figure 5B**), and required a lower insulin excursion (**Figure 5C**).
281 Crtc2 overexpression also improved insulin tolerance after fasting and weight loss (**Figure 5D**).
282 These effects were also apparent after 1 week of dox treatment in Crtc2 mice fed ad libitum (**Figure**
283 **S5A–C**). In primary myotubes, expression of Crtc2 was sufficient to significantly increase the uptake
284 of 2DG-glucose (**Figure 5E**).

285 Crtc2 mice and Crtc2/3-overexpressing myotubes upregulated a number of carbohydrate
286 signaling genes in normal fed conditions at both the RNA and protein levels (**Figure 5F–J**),
287 including the glucose transporter, *Glut4*, whose insulin-dependent translocation to the membrane
288 drives glucose uptake into skeletal muscle, accounting for 80% of glucose disposal. The *Nr4a1* gene
289 encodes Nur77, a nuclear receptor family transcription factor that regulates transcriptional programs

290 for carbohydrate metabolism, lipolysis, and mitochondrial biogenesis (48). *Irs2*, *Akt1*, and *Akt2*
291 encode core components of the insulin receptor signaling pathway that can coordinate anabolic
292 signaling and improve carbohydrate metabolism. We also validated a significant inhibition of
293 myogenin expression in the normal fed Crtc2 mice, a primary driver of muscle atrophy during
294 fasting. To validate on target mechanism of action, we generated stable cell lines overexpressing
295 Crtc3, dominant negative A-Creb, or dominant negative Crtc2 expressing only the Creb binding
296 domain (12). These results demonstrate that A-Creb and dn-Crtc3 blocked basal expression of Pgc-
297 1α, Irs2, and Akt2, and prevented phosphorylation of Akt1/2 at Thr308 (**Figure 5I–J**).

298 To test for pre-fasting changes in the central control of feeding and energy expenditure, we
299 completed a leptin infusion study, as leptin secretion from adipocytes both suppresses hunger and
300 stimulates the SNS. The WT and Crtc2 mice displayed identical patterns of weight loss following
301 leptin infusion (**Figure 5K**), and there were also no differences in plasma levels of feeding hormones,
302 cholesterol, or triglycerides (**Figure S5D–E**). Lastly, we considered that Crtc2 might be regulating
303 secreted proteins that modulate the response to dieting, using the Metazoan Secretome
304 Knowledgebase (49). Among 2,500 genes encoding likely secreted proteins, 171 DEGs were
305 regulated by Crtc2 during ADF. Using the Reactome.org peer-reviewed pathway database, we
306 detected significant enrichment of pathways regulating extracellular matrix, inter-cell signaling, and
307 immune function, among others (**Figure S5F**), but no changes in myokines that would drive weight
308 loss. However, Crtc2 signaling in skeletal muscle would be expected to have effects on other tissues
309 just from changes in metabolic flux, as Crtc2 mice displayed pre-fast increases in skeletal muscle
310 oxidative flux capacity.

311

312 **Discussion**

313 Skeletal muscle can be viewed as having semi-autonomous flux engines responding to a variety of
314 homeostatic stresses including nutrient flux, hormones, and exercise. We demonstrated here, and in
315 our previous study, that Crtc2/Creb1 signaling in skeletal muscle globally coordinates many of the
316 anabolic and metabolic benefits of exercise through the combined regulation of a number of these
317 flux engines. Our transcriptional and metabolic profiling revealed a profound effect of Crtc2 activity
318 that prevented the ADF-dependent loss of mitochondrial electron transport chain gene expression
319 and maintained energy expenditure (**Figures 2–3**). Pre-fast, Crtc2 stimulated mitochondrial
320 biogenesis and activity, upregulated β-oxidation genes, increased lipid flux capacity, and improved
321 insulin sensitivity and glucose disposal before and during fasting (**Figures 4–5**). While altered
322 mitochondrial function is the most likely mechanism explaining increased oxygen consumption and
323 maintenance of energy expenditure during fast, we did not examine whether Crtc2 regulated aerobic
324 glycolysis. While PGC-1α is sufficient to upregulate mitochondrial biogenesis, it does not replicate
325 the effects of exercise on energy expenditure Additionally, the previously reported increases in
326 skeletal muscle storage of glycogen and triglycerides also likely contributed to the early response,
327 perhaps explaining the initially slower rate of increased food consumption in the Crtc2 mice, while
328 the WT mice rapidly increased food intake to maintain weight. (**Figure 1E**). Changes in muscle
329 metabolic capacity may favor energy mobilization from tissues other than skeletal muscle. However,
330 when we looked at the obvious signaling pathways recruited by fasting, like leptin signaling, we
331 found no difference in leptin sensitivity.

332 It is not clear whether high- or moderate-intensity exercise is better for weight loss or insulin
333 sensitivity (50, 51). However, there is a clear effect of exercise dose on the amount of fat and weight
334 loss and cardiorespiratory health (52, 53), highlighting the importance of regular exercise for human
335 health. Exercise also improves the utilization of fat for fuel, which we observed here. A recent NIH

336 working group on obesity and exercise concluded that exercise intervention trials may have failed to
337 show an effect of exercise on long-term weight loss due to compliance issues, but it is very clear that
338 people who effectively maintain long-term weight loss exercise regularly (5, 54). These
339 transcriptional and metabolic adaptations may also explain how exercise increases energy
340 expenditure beyond that required during and immediately after completion of the exercise and alter
341 substrate utilization. Exercised calorie-restricted (CR) mice respond to refeeding by preferentially
342 oxidizing lipids, while using additional energy to refill fat stores by *de novo* lipogenesis (55). In
343 contrast, sedentary CR mice store fat more efficiently for rapid weight regain (55). This parallels the
344 effects of Crtc2 overexpression on the preferential loss of fat mass during ADF, similar to the effects
345 seen in humans who exercise during weight loss (21).

346 In skeletal muscle, adenylate cyclase/cAMP signaling is activated by several exercise-
347 regulated receptors, including GPCRs such as the β-adrenergic receptor (βAR) which is activated
348 by the SNS, the cholinergic receptor activated at the neuromuscular junction to induce calcium-
349 mediated muscle contraction, and receptors for adenosine and calcitonin gene-related peptide
350 (CGRP), which cause vasodilation during exercise (56, 57). We previously demonstrated in mice
351 that exercise-induced expression of the Creb1 target genes, *Ppargc1a*/PGC-1α and *Sik1*, and that
352 this transcriptional output was reversed by βAR blocker administration (13).

353 This work reveals mechanisms through which diet and exercise regulate substrate mobilization
354 and metabolism and highlights how these lifestyle modifications can alter mitochondrial function
355 and energy expenditure. Reduced energy expenditure and increased hunger during fasting are partly
356 mediated by a lowering of the satiety hormone leptin, which acts centrally to stimulate the SNS (2-
357 4). Leptin also secreted basally from adipose tissue in proportion to fat mass, so it is chronically
358 lower during fasting, which lowers sympathetic tone and energy expenditure, along with reductions

359 in circulating thyroid hormone and stimulating the HPA axis (**Figure 6A**). Within skeletal muscle,
360 increased glucocorticoids and AMPK activity are sufficient to reduce mitochondrial potential
361 (**Figure 3)**, which along with likely contributions from fasting-induced lowering of thyroid hormone,
362 βAR, and insulin receptor activity, induce mitochondrial dynamics and mitophagy (**Figure 6A**).

363 These energetic effects are reversed by exercise (**Figure 6B**), which we now show can be
364 recapitulated by enforced expression of Crtc2/Creb1 and upregulation of mitochondrial biogenesis
365 master regulatory genes, *Nr4a1*, *Nr4a3*, *Essrra*/ERRα, and *Ppargc1a*/PGC-1α (**Figure 5**).
366 overexpression of PGC-1α increases mitochondrial density and exercise performance, but without
367 the increase in metabolic rate that can occur from exercise training (58-61), highlighting the
368 coordination with other exercised-induced signaling pathways. The combination of βAR and Ca^{2+}
369 signaling are required to maximally stimulate nuclear translocation of Crtc2 in skeletal muscle (13).
370 In this model, increased GC and AMPK activity during exercise promotes mitochondrial dynamics,
371 which is then coupled with mitochondrial biogenesis to increase mitochondrial potential and mass,
372 in coordination with other metabolic changes (**Figures 4–5**). Overexpression of Crtc2 circumvented
373 the neuronal activation of Creb1, as Crtc2 mice had most of the hallmarks of exercise adaptations
374 before fasting and weight loss (**Figures 4–5, Figure S5B–C**) (13).

375

376
377
378 **Acknowledgements**. N.E.B. was supported by the BallenIsles Men's Golf Association. J.C.N. was
379 supported by the Frenchman's Creek Women for Cancer Research.

380

381 **Author contributions** Conceptualization, N.E.B., M.D.C., K.W.N.; Methodology, N.E.B., M.D.C.;
382 Investigation, N.E.B., J.C.N., S.S., R.H., D.S.; Writing – Original Draft, K.W.N., N.E.B., M.D.C.,

383 S.H., S.S.S.; Writing – Revision, K.W.N, J.C.N. ,N.E.B. Supervision, M.D.C, G.L.H., K.W.N.,

384 S.S.S., N.E.B.

385

386

387 **References**

388 1. C. L. Melby, H. L. Paris, R. M. Foright, J. Peth, Attenuating the Biologic Drive for Weight
389 Regain Following Weight Loss: Must What Goes Down Always Go Back Up? *Nutrients* **9**
390 (2017).
391 2. M. Rosenbaum *et al.*, Effects of experimental weight perturbation on skeletal muscle work
392 efficiency in human subjects. *Am J Physiol Regul Integr Comp Physiol* **285**, R183-192
393 (2003).
394 3. L. J. Arone, R. Mackintosh, M. Rosenbaum, R. L. Leibel, J. Hirsch, Autonomic nervous
395 system activity in weight gain and weight loss. *Am J Physiol* **269**, R222-225 (1995).
396 4. M. Rosenbaum *et al.*, Low-dose leptin reverses skeletal muscle, autonomic, and
397 neuroendocrine adaptations to maintenance of reduced weight. *J Clin Invest* **115**, 3579-
398 3586 (2005).
399 5. R. M. Foright *et al.*, Is regular exercise an effective strategy for weight loss maintenance?
400 *Physiol Behav* **188**, 86-93 (2018).
401 6. P. S. MacLean *et al.*, Regular exercise attenuates the metabolic drive to regain weight after
402 long-term weight loss. *Am J Physiol Regul Integr Comp Physiol* **297**, R793-802 (2009).
403 7. Y. Turk *et al.*, High intensity training in obesity: a Meta-analysis. *Obesity science &*
404 *practice* **3**, 258-271 (2017).
405 8. A. Mourier *et al.*, Mobilization of visceral adipose tissue related to the improvement in
406 insulin sensitivity in response to physical training in NIDDM. Effects of branched-chain
407 amino acid supplements. *Diabetes care* **20**, 385-391 (1997).
408 9. M. Rosenbaum *et al.*, Resistance Training Reduces Skeletal Muscle Work Efficiency in
409 Weight-Reduced and Non-Weight-Reduced Subjects. *Obesity (Silver Spring)* **26**, 1576-
410 1583 (2018).
411 10. D. M. Ostendorf *et al.*, Physical Activity Energy Expenditure and Total Daily Energy
412 Expenditure in Successful Weight Loss Maintainers. *Obesity (Silver Spring)* **27**, 496-504
413 (2019).
414 11. D. A. Walsh, J. P. Perkins, E. G. Krebs, An adenosine 3',5'-monophosphate-dependant
415 protein kinase from rabbit skeletal muscle. *The Journal of biological chemistry* **243**, 3763-
416 3765 (1968).
417 12. R. A. Screaton *et al.*, The CREB coactivator TORC2 functions as a calcium- and cAMP-
418 sensitive coincidence detector. *Cell* **119**, 61-74 (2004).
419 13. N. E. Bruno *et al.*, Creb coactivators direct anabolic responses and enhance performance
420 of skeletal muscle. *The EMBO journal* **33**, 1027-1043 (2014).
421 14. T. H. Ch'ng *et al.*, Activity-dependent transport of the transcriptional coactivator CRTC1
422 from synapse to nucleus. *Cell* **150**, 207-221 (2012).
423 15. P. S. Baxter, M. A. Martel, A. McMahon, P. C. Kind, G. E. Hardingham, Pituitary
424 adenylate cyclase-activating peptide induces long-lasting neuroprotection through the
425 induction of activity-dependent signaling via the cyclic AMP response element-binding
426 protein-regulated transcription co-activator 1. *J Neurochem* **118**, 365-378 (2011).
427 16. M. Taub, S. Garimella, D. Kim, T. Rajkhowa, F. Cutuli, Renal proximal tubule Na,K-
428 ATPase is controlled by CREB-regulated transcriptional coactivators as well as salt-
429 inducible kinase 1. *Cell Signal* **27**, 2568-2578 (2015).

17. D. V. Popov, E. A. Lysenko, P. A. Makhnovskii, N. S. Kurochkina, O. L. Vinogradova, Regulation of PPARGC1A gene expression in trained and untrained human skeletal muscle. *Physiological reports* **5** (2017).
18. D. V. Popov *et al.*, Contractile activity-specific transcriptome response to acute endurance exercise and training in human skeletal muscle. *Am J Physiol Endocrinol Metab* **316**, E605-E614 (2019).
19. B. Egan *et al.*, Exercise intensity-dependent regulation of peroxisome proliferator-activated receptor coactivator-1 mRNA abundance is associated with differential activation of upstream signalling kinases in human skeletal muscle. *J Physiol* **588**, 1779-1790 (2010).
20. N. Brandt *et al.*, Impact of adrenaline and metabolic stress on exercise-induced intracellular signaling and PGC-1alpha mRNA response in human skeletal muscle. *Physiological reports* **4** (2016).
21. N. D. Knuth *et al.*, Metabolic adaptation following massive weight loss is related to the degree of energy imbalance and changes in circulating leptin. *Obesity (Silver Spring)* **22**, 2563-2569 (2014).
22. J. C. Kerns *et al.*, Increased Physical Activity Associated with Less Weight Regain Six Years After "The Biggest Loser" Competition. *Obesity (Silver Spring)* **25**, 1838-1843 (2017).
23. L. B. Becnel *et al.*, Nuclear Receptor Signaling Atlas: Opening Access to the Biology of Nuclear Receptor Signaling Pathways. *PLoS One* **10**, e0135615 (2015).
24. S. Liu *et al.*, Mice lacking TR4 nuclear receptor develop mitochondrial myopathy with deficiency in complex I. *Mol Endocrinol* **25**, 1301-1310 (2011).
25. S. Karanth, E. K. Zinkhan, J. T. Hill, H. J. Yost, A. Schlegel, FOXN3 Regulates Hepatic Glucose Utilization. *Cell Rep* **15**, 2745-2755 (2016).
26. Y. Liu, J. Li, Y. Shang, Y. Guo, Z. Li, CARM1 contributes to skeletal muscle wasting by mediating FoxO3 activity and promoting myofiber autophagy. *Exp Cell Res* **374**, 198-209 (2019).
27. A. Galmozzi *et al.*, Inhibition of class I histone deacetylases unveils a mitochondrial signature and enhances oxidative metabolism in skeletal muscle and adipose tissue. *Diabetes* **62**, 732-742 (2013).
28. U. Dressel *et al.*, A dynamic role for HDAC7 in MEF2-mediated muscle differentiation. *The Journal of biological chemistry* **276**, 17007-17013 (2001).
29. J. Boucher, A. Kleinridders, C. R. Kahn, Insulin receptor signaling in normal and insulin-resistant states. *Cold Spring Harb Perspect Biol* **6** (2014).
30. P. Pinton, R. Rizzuto, p66Shc, oxidative stress and aging: importing a lifespan determinant into mitochondria. *Cell Cycle* **7**, 304-308 (2008).
31. J. L. Major, M. Salih, B. S. Tuana, Interplay between the E2F pathway and beta-adrenergic signaling in the pathological hypertrophic response of myocardium. *J Mol Cell Cardiol* **84**, 179-190 (2015).
32. R. Goldsmith *et al.*, Effects of experimental weight perturbation on skeletal muscle work efficiency, fuel utilization, and biochemistry in human subjects. *Am J Physiol Regul Integr Comp Physiol* **298**, R79-88 (2010).
33. S. E. Calvo, K. R. Clauser, V. K. Mootha, MitoCarta2.0: an updated inventory of mammalian mitochondrial proteins. *Nucleic Acids Res* **44**, D1251-1257 (2016).
34. V. Giorgio *et al.*, Dimers of mitochondrial ATP synthase form the permeability transition pore. *Proc Natl Acad Sci U S A* **110**, 5887-5892 (2013).

35. A. S. Rambold, B. Kostelecky, N. Elia, J. Lippincott-Schwartz, Tubular network formation protects mitochondria from autophagosomal degradation during nutrient starvation. *Proc Natl Acad Sci U S A* **108**, 10190-10195 (2011).
36. V. Nasta, D. Suraci, S. Gourdoupis, S. Ciofi-Baffoni, L. Banci, A pathway for assembling [4Fe-4S](2+) clusters in mitochondrial iron-sulfur protein biogenesis. *FEBS J* 10.1111/febs.15140 (2019).
37. J. Liu *et al.*, Mitochondrial Dysfunction Launches Dexamethasone-Induced Skeletal Muscle Atrophy via AMPK/FOXO3 Signaling. *Mol Pharm* **13**, 73-84 (2016).
38. D. Ratman *et al.*, Chromatin recruitment of activated AMPK drives fasting response genes co-controlled by GR and PPARalpha. *Nucleic Acids Res* **44**, 10539-10553 (2016).
39. G. R. Steinberg *et al.*, Reduced glycogen availability is associated with increased AMPKalpha2 activity, nuclear AMPKalpha2 protein abundance, and GLUT4 mRNA expression in contracting human skeletal muscle. *Appl Physiol Nutr Metab* **31**, 302-312 (2006).
40. B. Dasgupta *et al.*, The AMPK beta2 subunit is required for energy homeostasis during metabolic stress. *Mol Cell Biol* **32**, 2837-2848 (2012).
41. B. R. Barnes *et al.*, The 5'-AMP-activated protein kinase gamma3 isoform has a key role in carbohydrate and lipid metabolism in glycolytic skeletal muscle. *The Journal of biological chemistry* **279**, 38441-38447 (2004).
42. C. Aguer *et al.*, Muscle uncoupling protein 3 overexpression mimics endurance training and reduces circulating biomarkers of incomplete beta-oxidation. *FASEB J* **27**, 4213-4225 (2013).
43. S. Zhang, M. W. Hulver, R. P. McMillan, M. A. Cline, E. R. Gilbert, The pivotal role of pyruvate dehydrogenase kinases in metabolic flexibility. *Nutr Metab (Lond)* **11**, 10 (2014).
44. J. C. Drake, R. J. Wilson, Z. Yan, Molecular mechanisms for mitochondrial adaptation to exercise training in skeletal muscle. *FASEB J* **30**, 13-22 (2016).
45. M. A. Pearen, G. E. Muscat, Minireview: Nuclear hormone receptor 4A signaling: implications for metabolic disease. *Mol Endocrinol* **24**, 1891-1903 (2010).
46. Z. Wu *et al.*, Transducer of regulated CREB-binding proteins (TORCs) induce PGC-1alpha transcription and mitochondrial biogenesis in muscle cells. *Proc Natl Acad Sci U S A* **103**, 14379-14384 (2006).
47. R. K. Conlee, M. J. Rennie, W. W. Winder, Skeletal muscle glycogen content: diurnal variation and effects of fasting. *Am J Physiol* **231**, 614-618 (1976).
48. M. A. Maxwell *et al.*, Nur77 regulates lipolysis in skeletal muscle cells. Evidence for cross-talk between the beta-adrenergic and an orphan nuclear hormone receptor pathway. *The Journal of biological chemistry* **280**, 12573-12584 (2005).
49. J. Meinken, G. Walker, C. R. Cooper, X. J. Min, MetazSecKB: the human and animal secretome and subcellular proteome knowledgebase. *Database (Oxford)* **2015** (2015).
50. S. E. Keating, N. A. Johnson, G. I. Mielke, J. S. Coombes, A systematic review and meta-analysis of interval training versus moderate-intensity continuous training on body adiposity. *Obes Rev* **18**, 943-964 (2017).
51. R. W. McGarrah, C. A. Slentz, W. E. Kraus, The Effect of Vigorous- Versus Moderate-Intensity Aerobic Exercise on Insulin Action. *Curr Cardiol Rep* **18**, 117 (2016).
52. T. S. Church, C. P. Earnest, J. S. Skinner, S. N. Blair, Effects of different doses of physical activity on cardiorespiratory fitness among sedentary, overweight or obese postmenopausal

521 women with elevated blood pressure: a randomized controlled trial. *JAMA* **297**, 2081-2091
522 (2007).
523 53. C. A. Slentz *et al.*, Effects of the amount of exercise on body weight, body composition,
524 and measures of central obesity: STRRIDE--a randomized controlled study. *Arch Intern*
525 *Med* **164**, 31-39 (2004).
526 54. P. S. MacLean *et al.*, NIH working group report: Innovative research to improve
527 maintenance of weight loss. *Obesity (Silver Spring)* **23**, 7-15 (2015).
528 55. A. J. Steig *et al.*, Exercise reduces appetite and traffics excess nutrients away from
529 energetically efficient pathways of lipid deposition during the early stages of weight regain.
530 *Am J Physiol Regul Integr Comp Physiol* **301**, R656-667 (2011).
531 56. R. Berdeaux, R. Stewart, cAMP signaling in skeletal muscle adaptation: hypertrophy,
532 metabolism, and regeneration. *Am J Physiol Endocrinol Metab* **303**, E1-17 (2012).
533 57. R. Rudolf *et al.*, Alterations of cAMP-dependent signaling in dystrophic skeletal muscle.
534 *Front Physiol* **4**, 290 (2013).
535 58. C. S. Choi *et al.*, Paradoxical effects of increased expression of PGC-1alpha on muscle
536 mitochondrial function and insulin-stimulated muscle glucose metabolism. *Proc Natl Acad*
537 *Sci U S A* **105**, 19926-19931 (2008).
538 59. M. Tadaishi *et al.*, Skeletal muscle-specific expression of PGC-1alpha-b, an exercise-
539 responsive isoform, increases exercise capacity and peak oxygen uptake. *PLoS One* **6**,
540 e28290 (2011).
541 60. R. P. Shook *et al.*, Moderate cardiorespiratory fitness is positively associated with resting
542 metabolic rate in young adults. *Mayo Clin Proc* **89**, 763-771 (2014).
543 61. M. Gilliat-Wimberly, M. M. Manore, K. Woolf, P. D. Swan, S. S. Carroll, Effects of
544 habitual physical activity on the resting metabolic rates and body compositions of women
545 aged 35 to 50 years. *J Am Diet Assoc* **101**, 1181-1188 (2001).
546

547

548 **Figure Legends**

549 **Figure 1. Crtc2/Creb1 signaling enables greater loss of weight and adiposity during alternate**
550 **day fasting (ADF).**

551 (**A**) Summary of previous work showing that Crtc2 overexpression produced an exercised
552 phenotype (13).

553 (**B**) 18-week old C57BL/6 male control (WT) and Crtc2 mice were treated with dox for 35 days
554 and weighed. Data are shown as box-and-whisker plot, indicating the middle quartiles and range.
555 *N* = 6 (WT) or 5 (Crtc2) mice per group.

556 (**C-F**) Mice from (**B**) were subject to alternate day fasting (ADF).

557 (**C**) Changes in the body weight during ADF.

558 (**D**) Weight regain after the ADF treatment and 3 weeks of ad libitum feeding. *significant in
559 Sidak's test for planned comparisons.

560 (**E**) Behaviors were assayed with Biodak monitoring system, including number of meals, bouts per
561 meal, meal duration, and kilocalories consumed over the 12-hr re-feeding period.

562 (**F**) Adiposity and lean mass determined by whole-body NMR measurements taken before and
563 after 8 cycles of ADF.

564 (**G**) 8-week old C57BL/6 male control and Crtc2 mice were treated with dox and placed on a high
565 fat diet (HFD). *N* = 9 (WT) or 7 (Crtc2) mice per group

566 Data are shown as mean ± SEM. See also **Figure S1**

567

568 **Figure 2. Transcriptional control of fasting and weight loss and its regulation by Crtc2.**

569 (**A**) Mice TA muscles were transduced with GFP control or Crtc2 expression vector. Crtc2 mRNA
570 levels in the TA of mice fed ad libitum (Fed), or subject to ADF (Fast) were compared by qPCR.

571 *N* = 3 mice per group.

572 (**B**) Venn diagram showing the numbers of DEGs identified by mRNA-seq comparing the effects
573 of ADF in control versus Crtc2-transduced TA muscles.

574 (**C**) Biological processes and functions regulated by ADF and Crtc2. Gene ontology (GO) analysis
575 suggests that ADF regulates several processes/ functions in a Crtc2-sensitive manner. The numbers
576 of DEGs involved in each process are shown. See SI Appendix, **Dataset S1** for a complete list of
577 represented GO annotations.

578 (**D**) Examples of ADF-regulated transcriptional programs and mRNAs in control TA muscles.

579 (**E–G**) Gene expression profiles in control and Crtc2-transduced TA muscles of mice subjected to
580 ADF relative to the ad libitum fed mice (columns 1–2), and effect of Crtc2 transduction relative to
581 control during ADF (column 3). Expression profiles of genes that encode **E**) nuclear receptors, **F**)
582 other transcription factors, and **G**) transcriptional coregulators. ADF-regulated genes in control
583 muscle appear in **bold**. *Crtc2-regulated genes in mice subjected to ADF. *ADF-regulated genes
584 in Crtc2-transduced muscle but not control. FC, fold change. Also see SI Appendix, **Dataset S1**

585

586 **Figure 3. Electron transport chain gene expression and whole-body energy expenditure**
587 **regulation by weight loss and fasting is reversed by Crtc2 expression.**

588 (**A**–**D**) Gene expression profiles in control and Crtc2-transduced TA muscles of mice subjected to
589 ADF relative to the ad libitum fed mice (columns 1–2), and effect of Crtc2 transduction relative to
590 control during ADF (column 3). The profiles of all genes encoding **A**) mitochondrial proteins,
591 including subunits of electron transport chain (ETC) complexes, **B**) subunits of the mitochondrial
592 ATPase (complex V), **C)** ribosomal subunits, and **D**) highlighted mitochondrial proteins, are
593 shown. ADF-regulated genes in control muscle appear in **bold**. *Crtc2-regulated genes in mice

594 subjected to ADF. *ADF-regulated genes in Crtc2-transduced muscle but not control. FC, fold
595 change.
596 (**E**) Effects of Dex on lean body mass. Mice injected with vehicle or 10 mg/kg Dex were fasted
597 overnight. Lean mass was measured by whole-body NMR before and after treatment. *N* = 5 mice
598 per group.
599 (**F**) Diameter and mitochondrial potential of steroid-deprived primary myotubes treated for 2 days
600 with vehicle or 100 nM Dex were compared by confocal high-content imaging. *N* = 24–27 images
601 x 50–100 myotubes per image.
602 (**G**) Steroid-deprived C2C12 myotubes were stimulated with 100 nM Dex for 0–12 h. Levels of
603 phosphorylated and total AMPK in whole lysates were compared by western blot.
604 (**H**) Diameter of steroid-deprived C2C12 myotubes treated for 48 h with vehicle, 100 nM Dex, or
605 1 uM AICAR were compared by confocal high content imaging. *N* = 24–27 images x 50–100
606 myotubes per image.
607 (**I**) Expression levels of genes encoding AMPK subunits in mice described in **Figure 2**.
608 (**J**) VO_2 and VCO_2 were measured continuously (**Figure S2A**) for 72 hrs. in a CLAMS animal
609 monitoring system. Shown are the 12-hr averages. *N* = 8 mice per group.
610 (**K**) Total energy expenditure was calculated from VO_2 and VCO_2 values using the Lusk equation.
611 Data are shown as mean ± SEM. Also see **Figure S3**
612
613 **Figure 4. Crtc2 expression in skeletal muscle enhances mitochondrial biogenesis.**
614 (**A**) Expression profiles of genes that regulate lipid metabolism in mice described in **Figure 2.**
615 (**B**) Histological analysis of succinate dehydrogenase in myofibers from gastrocnemius muscle
616 sections after dox treatment. Scale bar = 500 μm.

617 (**C**) Gene induction calculated relative to WT mice. *N* = 8 mice per group.

618 (**D**) Gene expression in primary myocytes transduced with adenovirus expressing Crtc2 or GFP

619 control 72 hr post-transduction.

620 (**E**) C2C12 myocytes were transduced with adenovirus GFP, Crtc2, or A-Creb genes and analyzed

621 by confocal high content imaging. *N* = 24–27 images x 50–100 myotubes per image.

622 (**F**) Crtc2 expression plasmid was electroporated into the tibialis anterior muscle and GFP plasmid

623 in the contralateral leg. After 7 days, DNA was extracted for assessment of mitochondrial DNA

624 (mt-DNA) for Crtc2/GFP control. *N* = 5 mice per group.

625 (**G**) Oxidation of ^{3}H-Palmitic acid in the supernatant of primary myocytes transduced with control,

626 Crtc2, or Crtc3-expressing adenovirus.

627 * $p < 0.05$. Data are shown as mean + SEM. **See also Figure S4**

628

629 **Figure 5. Crtc2 transgenic mice maintain enhanced glucose disposal and insulin tolerance**

630 (**A**) Expression profiles of genes that regulate carbohydrate metabolism in mice described in

631 **Figure 2**.

632 (**B**) Glucose tolerance test (GTT) after alternate day fasting. Right panel, area under the curve. *N*

633 = 10 mice per group

634 (**C**) Plasma insulin levels during GTT described in panel **B**.

635 (**D**) Insulin tolerance tests after 8 cycles of ADF. *N* = 10 mice per group

636 (**E**) Insulin-mediated uptake of 2-deoxy-D-glucose in primary myocytes transduced with

637 adenovirus expressing Crtc2 or GFP control. *N* = 10 per group. Student's t-test.

638 (**F**) Crtc2 mice were treated +/- dox for 1 week and the gene induction compared by qPCR relative

639 to the no dox groups. N= 10 per group.

640 (**G**) Gene expression in primary myocytes transduced with adenovirus expressing Crtc2 or GFP
641 control were compared by qPCR. *N*=4 per group.
642 (**H**) Western blot of whole lysates from primary myocytes transduced with the indicated plasmids.
643 (**I–J**) Myocytes stably expressing GFP, Crtc3 (lanes 2 and 3), dominant negative Creb (A-CREB),
644 or dominant negative Crtc2 (dn-Crtc) were compared by western blots.
645 (**K**) WT or Crtc2 mice were injected twice daily with 0.5 mg/kg leptin and weight was monitored.
646 *N*=8 mice per group.
647 Data are mean ± SEM. **See also Figure S5.**
648
649 **Figure 6. Hormonal and neural modulation of energy expenditure in skeletal muscle**
650 (**A**) Fasting-induced regulation of mitochondrial dynamics and mitophagy.
651 (**B**) Exercise-induced regulation of mitochondrial dynamics and mitochondrial biogenesis, which
652 can be constitutively activated by overexpression of Crtc2 in skeletal muscle.
653 bAR, b-adrenergic receptor; GR, glucocorticoid receptor; HPA, hypothalamic-pituitary-adrenal axis;
654 HPT, hypothalamic-pituitary-thyroid axis; InsR, insulin receptor; nAchR, nicotinic acetylcholine
655 receptor; SNS, sympathetic nervous system; TH, thyroid hormone
656
657

658 **Materials and Methods**

659 **Statistical analyses**

660 Changes in body weight and body were analyzed with 2-way analysis of variance. For VO_2,
661 respiratory quotient, and ambulation data, the ad libitum and fasted periods were analyzed
662 separately with 2-way ANOVA, and the refeeding data analyzed with Student's T-test. For the
663 energy consumption data, the fasted and re-fed data were analyzed together with 2-way ANOVA.
664 Gene expression data were analyzed with 1-way ANOVA, with Dunnett's test for multiple
665 comparisons of each gene to its corresponding control. Glycemia and insulin changes over time
666 were analyzed with 2-way ANOVA, and the AUC assessed with Student's T-test. The behavioral
667 data for meal consumption were analyzed with Student's T-tests.

668

669 **Crtc2 transgenic mice and animal care**

670 All animal procedures were approved by the Scripps Research Institute ICACUC. TRE-Crtc2^{tm}
671 mice were generated by cloning FLAG-Crtc2 (S171A, S275A, K628R) into pTRE-Tight. Oocyte
672 injections were conducted into C57Bl6 at the University of Cincinnati. Double transgenic mice
673 (DTg) were generated by crossing C57BL/6-Tg(TRE-Crtc2tm)1Mdc/j mice with 1256[3Emut]
674 MCK-rtTA transgenic mice, which expresses the reverse tetracycline transactivator (rtTA)
675 regulated by the 1256[3Emut] MCK promoter specifically in skeletal muscle (Grill *et al*, 2003).
676 Wild type and TRE littermates were used as controls and treated with DOX in the same manner as
677 DTg mice. High fat diet (Research Diet D12450J) contained 60 kcal% fat and matched control low
678 fat diet (D12492) contained 10kCal% fat and 7% sucrose.

679

680

681

682 **Data Availability**

683 The raw and processed RNA-seq dataset is freely available to the public at the National Center for
684 Biotechnology Information (NCBI) Gene Expression Omnibus (GEO)
685 https://www.ncbi.nlm.nih.gov/geo/ and can be retrieved with the accession number GSE149150,
686 which will be released upon publication of this manuscript. The processed RNA-seq dataset is also
687 provided in SI Appendix, **Dataset S1**. Relevant protocols and raw data not detailed in the Methods
688 or Supplementary Information are available upon request.

689

690

691

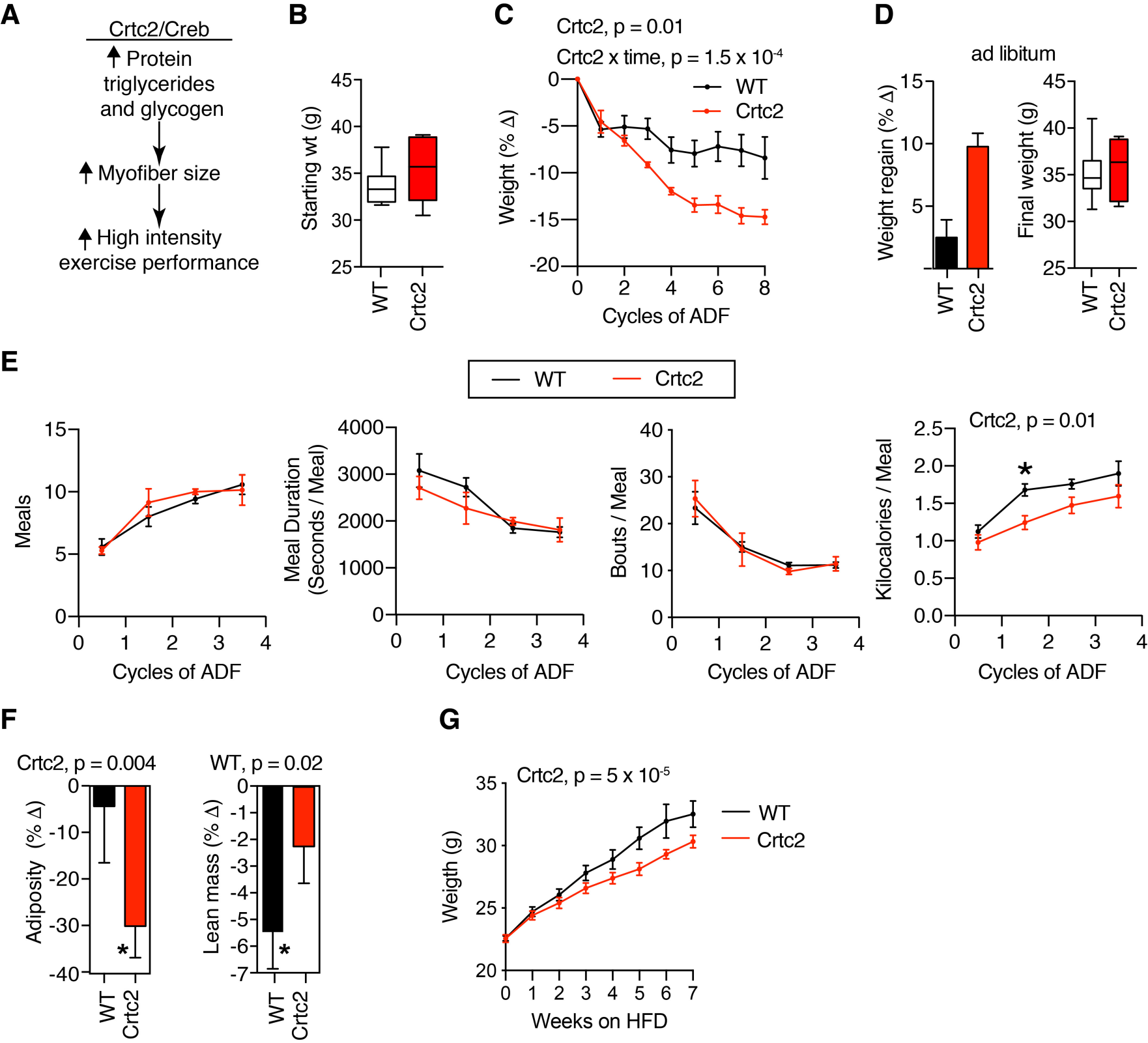
A
Crtc2/Creb
Protein triglycerides and glycogen
Myofiber size
High intensity exercise performance
B
Starting wt (g)
WT
Crtc2
C
Crtc2, p = 0.01
Crtc2 x time, p = 1.5 x 10-4
Weight (% Δ)
Cycles of ADF
D
ad libitum
Weight regain (% Δ)
Final weight (g)
E
Meals
Meal Duration (Seconds / Meal)
Bouts / Meal
Kilocalories / Meal
Crtc2, p = 0.01
F
Crtc2, p = 0.004
WT, p = 0.02
Adiposity (% Δ)
Lean mass (% Δ)
G
Crtc2, p = 5 x 10-5
Weigth (g)
Weeks on HFD

Figure 1

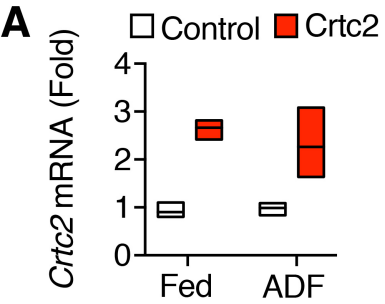

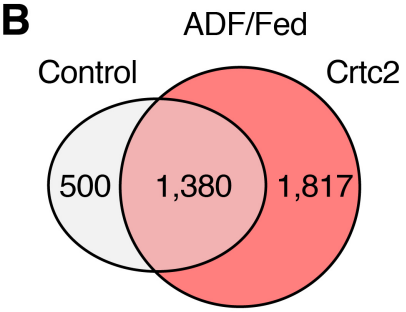

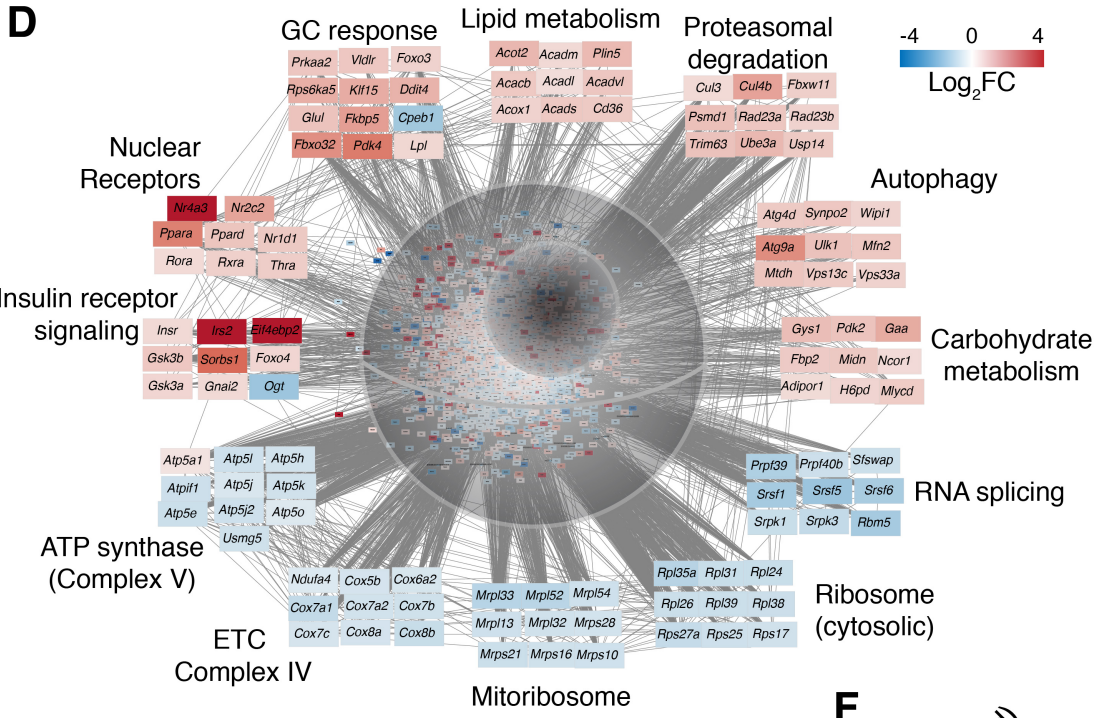

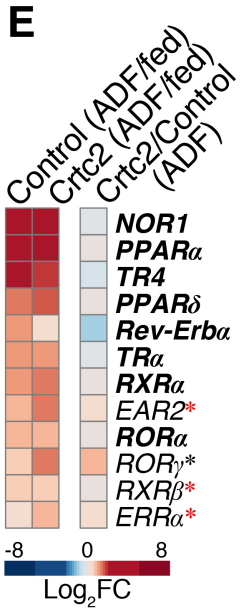

C

Biological process/function — No. of DEGs — *Crtc2 regulated >20% of DEGs

Source	GO term	Total	Regulated by ADF: Control	Regulated by ADF: Crtc2	Regulated by ADF: Both	Crtc2/ Control (fasted)
M.E. Pipkin	Transcription factors	324	155	284	124	42
EpiFactors	Coregulators	154	84	135	68	14
GO:0042255	Ribosome assembly	20	16	15	11	2
NURSA	Nuclear hormone receptors (NHRs)	13	8	11	6	1
GO:0006629	Lipid metabolic process	258	128	223	103	43
GO:0006635	Fatty acid beta-oxidation	26	16	22	13	4
GO:0008286	Insulin receptor signaling pathway	37	25	32	21	6
Kuo et al.	Glucocorticoid response	1,145	563	980	436	192
GO:0043161	Proteasomal protein degradation	104	57	91	46	9
GO:0000502	Proteasome complex	30	21	26	17	0
GO:0006914	Autophagy	105	59	98	52	13
GO:0042752	Regulation of circadian rhythm	22	14	19	11	4
GO:0004672	Protein kinase activity	133	65	127	62	22
GO:0008380	RNA splicing	71	50	61	42	3
GO:0003009	Skeletal muscle contraction	20	14	18	12	1
GO:0042594	Response to starvation	37	23	36	23	2
GO:0005746	Mitochondrial respiratory chain	51	42	14	8	23*
MitoCarta2.0	Mitochondrial proteins	368	220	246	116	78*
GO:0030433	Ub-dependent ERAD pathway	26	11	23	9	5
GO:0006954	Inflammatory response	105	30	86	17	41*
GO:0006468	Protein phosphorylation	385	174	339	140	91*
GO:0007249	I-kappaB kinase/NF-kappaB cascade	53	18	46	13	12*

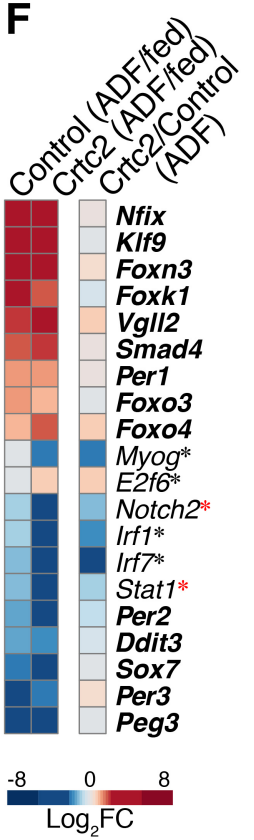

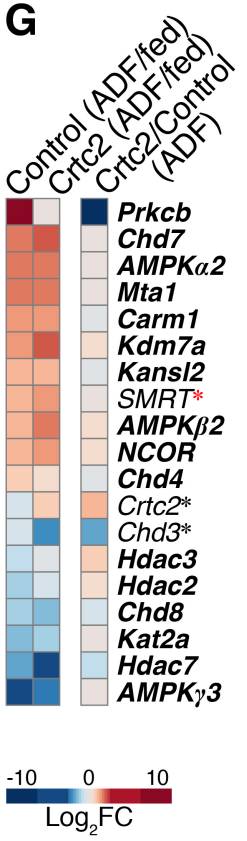

Figure 2

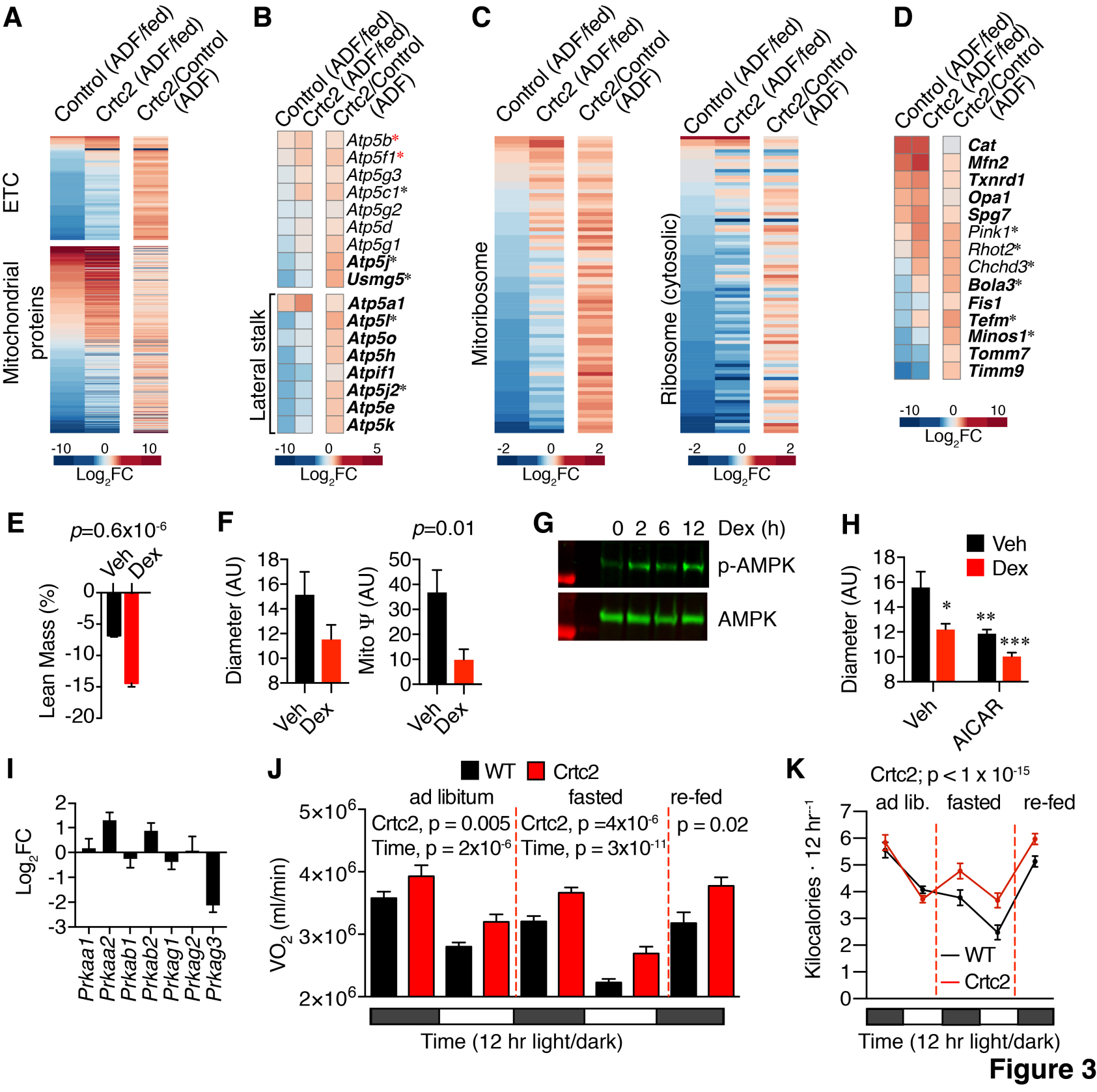
A
Control (ADF/fed)
Crtc2 (ADF/fed)
Crtc2/Control (ADF)
ETC
Mitochondrial proteins
-10 0 10
Log2FC
B
Atp5b*
Atp5f1*
Atp5g3
Atp5c1*
Atp5g2
Atp5d
Atp5g1
Atp5j*
Usmg5*
Lateral stalk
Atp5a1
Atp5l*
Atp5o
Atp5h
Atpif1
Atp5j2*
Atp5e
Atp5k
-10 0 5
Log2FC
C
Mitoribosome
Ribosome (cytosolic)
-2 0 2
Log2FC
D
Cat
Mfn2
Txnrd1
Opa1
Spg7
Pink1*
Rhot2*
Chchd3*
Bola3*
Fis1
Tefm*
Minos1*
Tomm7
Timm9
-10 0 10
Log2FC
E
p=0.6x10-6
Veh
Dex
Lean Mass (%)
0 -5 -10 -15 -20
F
p=0.01
Diameter (AU)
18 16 14 12 10 8
Mito Ψ (AU)
50 40 30 20 10 0
Veh
Dex
G
0 2 6 12 Dex (h)
p-AMPK
AMPK
H
Veh
Dex
Diameter (AU)
18 16 14 12 10 8
*
**
***
Veh
AICAR
I
Log2FC
2 1 0 -1 -2 -3
Prkaa1
Prkaa2
Prkab1
Prkab2
Prkag1
Prkag2
Prkag3
J
WT
Crtc2
ad libitum
fasted
re-fed
Crtc2, p = 0.005
Time, p = 2x10-6
Crtc2, p =4x10-6
Time, p = 3x10-11
p = 0.02
VO2 (ml/min)
5×10^6
4×10^6
3×10^6
2×10^6
Time (12 hr light/dark)
K
Crtc2; p < 1 x 10-15
ad lib.
fasted
re-fed
Kilocalories · 12 hr-1
7 6 5 4 3 2 1 0
WT
Crtc2
Time (12 hr light/dark)

Figure 3

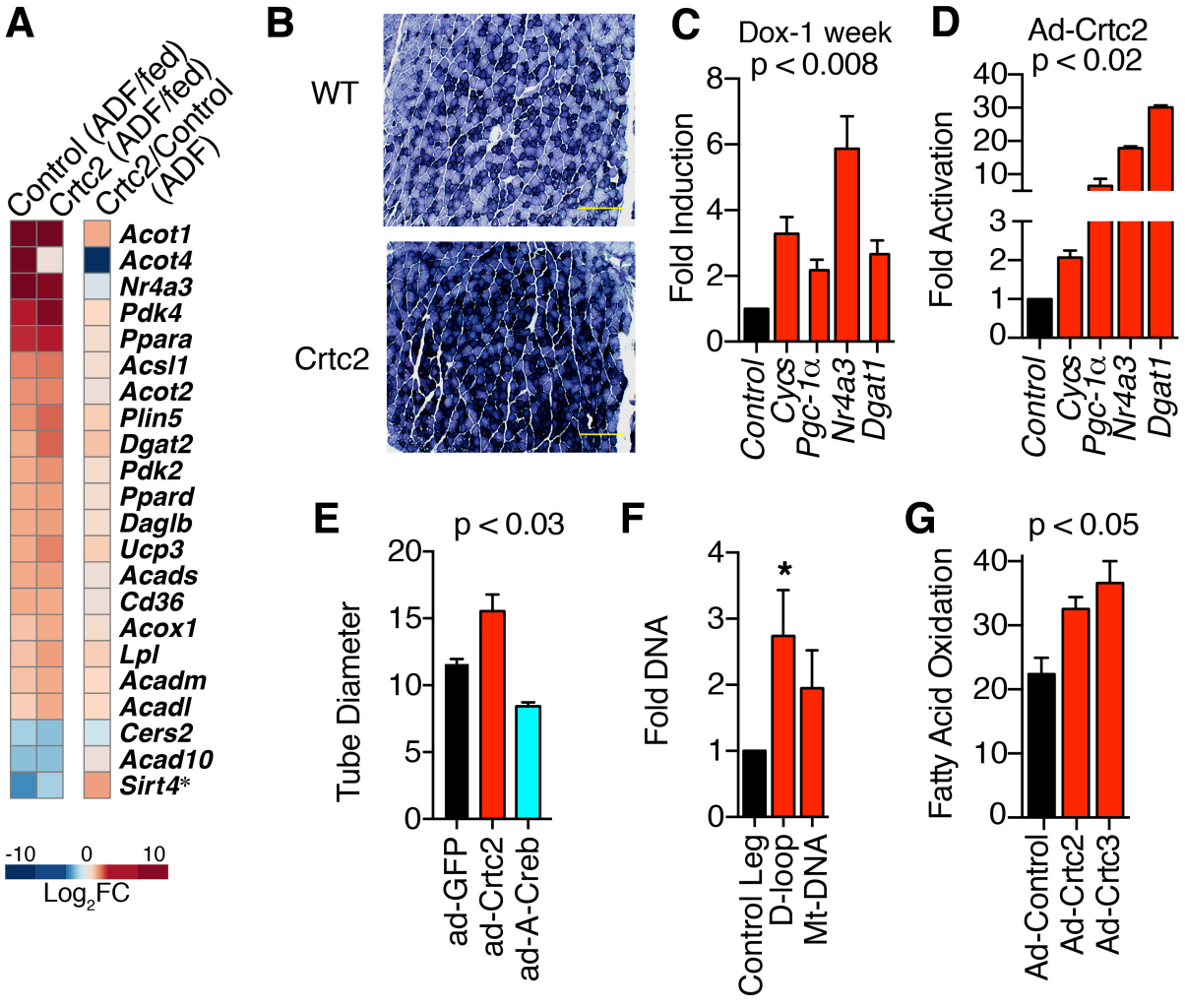
A
Control (ADF/fed)
Crtc2 (ADF/fed)
Crtc2/Control (ADF)
Acot1
Acot4
Nr4a3
Pdk4
Ppara
Acsl1
Acot2
Plin5
Dgat2
Pdk2
Ppard
Daglb
Ucp3
Acads
Cd36
Acox1
Lpl
Acadm
Acadl
Cers2
Acad10
Sirt4*
-10
0
10
Log2FC
B
WT
Crtc2
C
Dox-1 week
p < 0.008
Fold Induction
Control
Cycs
Pgc-1α
Nr4a3
Dgat1
D
Ad-Crtc2
p < 0.02
Fold Activation
Control
Cycs
Pgc-1α
Nr4a3
Dgat1
E
p < 0.03
Tube Diameter
ad-GFP
ad-Crtc2
ad-A-Creb
F
Fold DNA
*
Control Leg
D-loop
Mt-DNA
G
p < 0.05
Fatty Acid Oxidation
Ad-Control
Ad-Crtc2
Ad-Crtc3

Figure 4

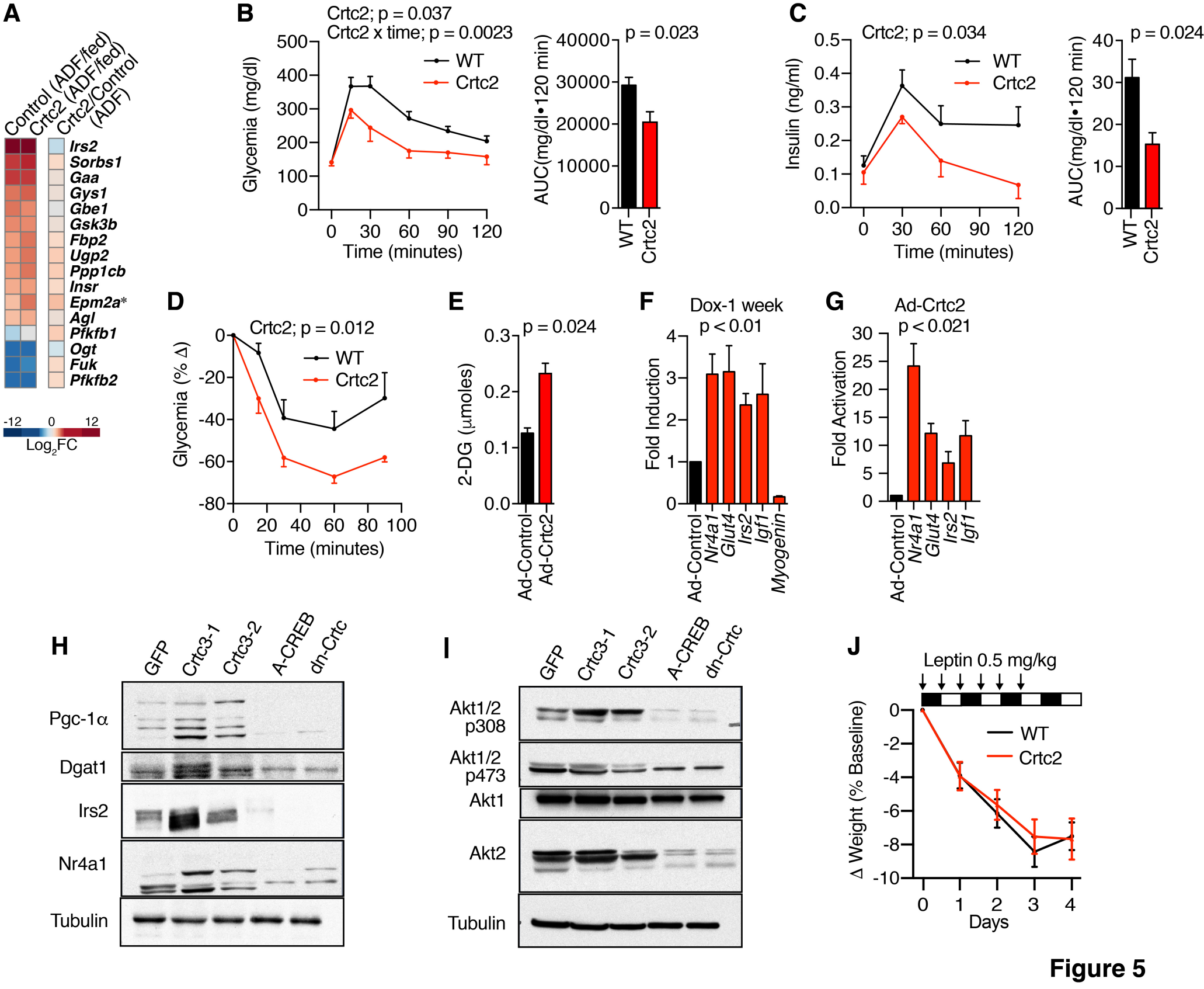
A
Control (ADF/fed)
Crtc2 (ADF/fed)
Crtc2/Control (ADF)
Irs2
Sorbs1
Gaa
Gys1
Gbe1
Gsk3b
Fbp2
Ugp2
Ppp1cb
Insr
Epm2a*
Agl
Pfkfb1
Ogt
Fuk
Pfkfb2
-12
0
12
Log2FC
B
Crtc2; p = 0.037
Crtc2 x time; p = 0.0023
WT
Crtc2
Glycemia (mg/dl)
Time (minutes)
p = 0.023
AUC(mg/dl•120 min)
C
Crtc2; p = 0.034
Insulin (ng/ml)
p = 0.024
D
Crtc2; p = 0.012
Glycemia (% Δ)
E
p = 0.024
2-DG (μmoles)
Ad-Control
Ad-Crtc2
F
Dox-1 week
p < 0.01
Fold Induction
Nr4a1
Glut4
Irs2
Igf1
Myogenin
G
Ad-Crtc2
p < 0.021
Fold Activation
H
GFP
Crtc3-1
Crtc3-2
A-CREB
dn-Crtc
Pgc-1α
Dgat1
Irs2
Nr4a1
Tubulin
I
Akt1/2 p308
Akt1/2 p473
Akt1
Akt2
Tubulin
J
Leptin 0.5 mg/kg
Δ Weight (% Baseline)
Days

Figure 5

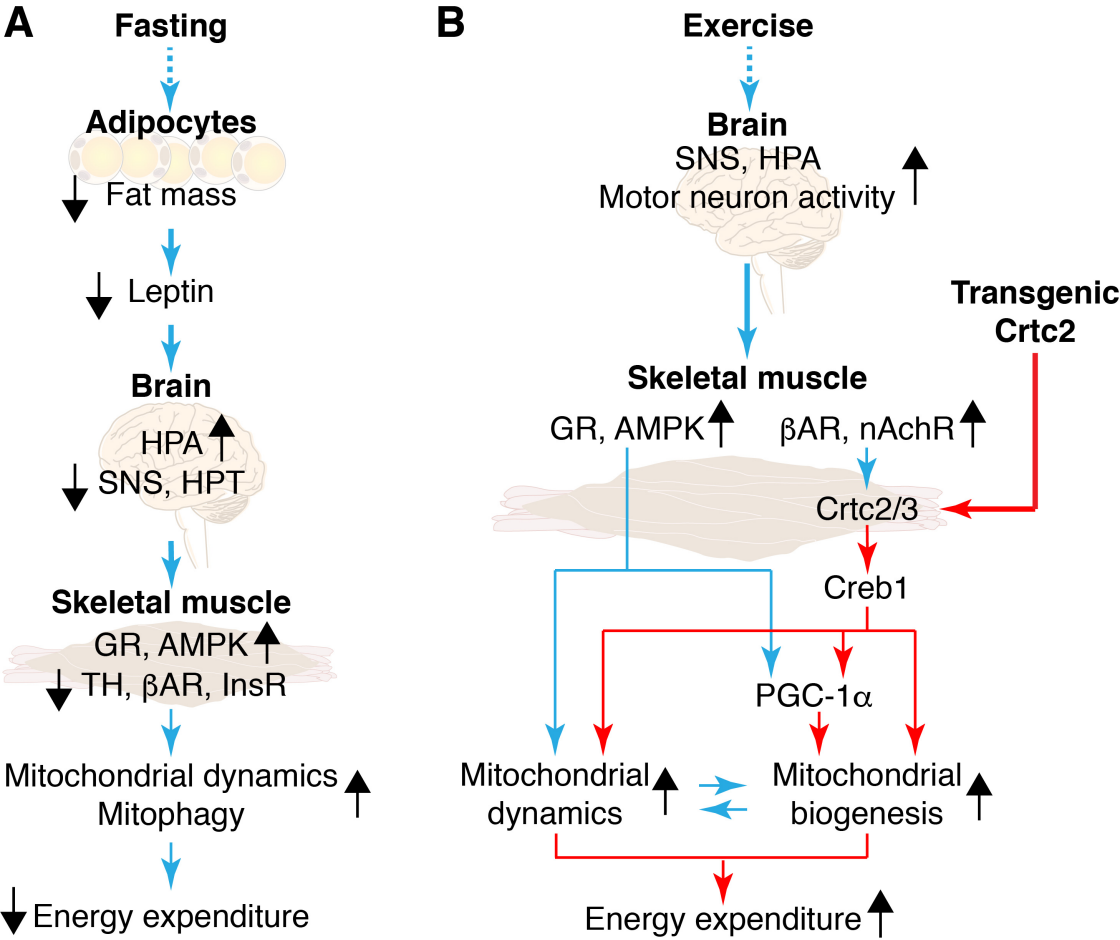
A
Fasting
Adipocytes
Fat mass
Leptin
Brain
HPA
SNS, HPT
Skeletal muscle
GR, AMPK
TH, βAR, InsR
Mitochondrial dynamics
Mitophagy
Energy expenditure
B
Exercise
Brain
SNS, HPA
Motor neuron activity
Transgenic
Crtc2
Skeletal muscle
GR, AMPK
βAR, nAchR
Crtc2/3
Creb1
PGC-1α
Mitochondrial
dynamics
Mitochondrial
biogenesis
Energy expenditure

Figure 6